



A screen-printed paper microbial fuel cell biosensor for detection of toxic compounds in water

Jon Chouler^{a,b}, Álvaro Cruz-Izquierdo^c, Saravanan Rengaraj^a, Janet L. Scott^c,
Mirella Di Lorenzo^{a,*}

^a Department of Chemical Engineering, University of Bath, Bath BA2 7AY, United Kingdom

^b EPSRC Centre for Doctoral Training in Sustainable Chemical Technologies, University of Bath, Bath BA2 7AY, United Kingdom

^c Department of Chemistry, University of Bath, Bath BA2 7AY, United Kingdom



ARTICLE INFO

Keywords:

Microbial fuel cell
Biosensor
Paper electronics
Water quality
Formaldehyde

ABSTRACT

Access to safe drinking water is a human right, crucial to combat inequalities, reduce poverty and allow sustainable development. In many areas of the world, however, this right is not guaranteed, in part because of the lack of easily deployable diagnostic tools. Low-cost and simple methods to test water supplies onsite can protect vulnerable communities from the impact of contaminants in drinking water. Ideally such devices would also be easy to dispose of so as to leave no trace, or have a detrimental effect on the environment. To this aim, we here report the first paper microbial fuel cell (pMFC) fabricated by screen-printing biodegradable carbon-based electrodes onto a single sheet of paper, and demonstrate its use as a shock sensor for bioactive compounds (e.g. formaldehyde) in water. We also show a simple route to enhance the sensor performance by folding back-to-back two pMFCs electrically connected in parallel. This promising proof of concept work can lead to a revolutionizing way of testing water at point of use, which is not only green, easy-to-operate and rapid, but is also affordable to all.

1. Introduction

The provision of clean water is essential to allow economic growth and environmental sustainability (WWAP (United Nations World Water Assessment Programme), 2015). Nonetheless, in many poor areas of the world, access to safe water is still a luxury (Ongley, 2001). In countries that lack suitable infrastructure, the assessment of water quality is a real challenge (Sarpong Adu-manu et al., 2017). Along with effective sanitation and wastewater treatment programs, it is extremely important to establish methods for water quality analysis that do not require expensive laboratory equipment and/or skilled personnel yet provide rapid response and have onsite functionality (Palaniappan et al., 2010).

In recent years, microbial fuel cell (MFC) technology has demonstrated promising potential as a tool for water quality monitoring (Chouler and Di Lorenzo, 2015). MFCs are devices that directly convert the chemical energy contained in organic matter into electricity via the metabolic processes of microorganisms (Allen and Bennetto, 1993; Potter, 1911). On the anode surface of these devices, a biofilm develops,

which contains electroactive bacteria capable of extracellularly transferring the electrons they generate from the oxidation of organic compounds to the electrode. The current generated by MFCs can, therefore, be directly related to the metabolic activity of these anodic bacteria (Di Lorenzo et al., 2014). Any disturbances to their metabolic pathways, caused by environmental changes, such as organic load, or the sudden presence of a bioactive and toxic compound, are translated into a change in the electricity generated (Di Lorenzo et al., 2009; Stein et al., 2010). This is the principle behind the use of MFCs as a tool to detect the presence of toxicants in water (Jiang et al., 2015). The major advantage of MFC-based sensors for water quality monitoring over other devices suggested in the literature is their simplicity. In MFCs, the anodic biofilm functions as the recognition component (Chouler and Di Lorenzo, 2015). Its response to the presence of a toxicant causes a change in the rate of flow of electrons to the anode (the transducer), thus generating a measurable change in the output current. As such, there is no need for expensive external equipment that acts as a transducer, as is required in many other types of sensors proposed (Mulchandani et al., 1998; Vaiopoulou et al., 2005).

Abbreviations: AW, artificial wastewater; cpMFC, chitosan doped paper-based microbial fuel cell; CV, cyclic voltammetry; DMSO, dimethyl sulfoxide; EIS, electrochemical impedance spectroscopy; EMIMAc, 1-, ethyl-3-methylimidazolium; fpMFC, folded paper-based microbial fuel cell; HPLC, High-performance liquid chromatography; LSV, linear sweep voltammetry; MFC, microbial fuel cell; OCV, open circuit voltage; PBS, phosphate buffer solution; pMFC, paper-based microbial fuel cell; SEM, scanning electron microscope

* Corresponding author.

E-mail address: M.Di.Lorenzo@bath.ac.uk (M. Di Lorenzo).

<http://dx.doi.org/10.1016/j.bios.2017.11.018>

Received 2 September 2017; Received in revised form 11 October 2017; Accepted 2 November 2017

Available online 06 November 2017

0956-5663/ © 2017 The Authors. Published by Elsevier B.V. This is an open access article under the CC BY license (<http://creativecommons.org/licenses/by/4.0/>).

Nomenclature		P	Power (W)
a	Gradient of glycolic acid calibration curve (mL mg^{-1})	PA	Peak area (-)
b	intercept of glycolic acid calibration curve (-)	R	Resistance (Ω)
DF	dilution factor	V	Voltage (V)
I	Current (A)	WOF_{ini}	Initial weight of paper sample (mg)

Despite their promise, practical implementation of MFCs as sensors is still restricted by the use of expensive manufacturing materials (Winfield et al., 2015) and device designs that are not suitable for portable applications, due to the need for pumps and tubing during operation (Hashemi et al., 2016). All these aspects reflect in an increase in both capital and operating costs. There is therefore a great need for innovative and cost-effective MFC designs.

Recently, paper electronics, which refer to the use of paper as a functional part of the electronic components of a device, are attracting increasing attention (Zhao and van den Berg, 2008). The use of paper can lead to the development of innovative, light and recyclable electronics, with the added benefits of cost-effectiveness, facile operation, easy disposal after use, ready portability and widespread availability (Yetisen et al., 2013). Paper has been explored for the fabrication of MFCs to generate energy from urine (Winfield et al., 2015) and tryptic soy broth (Hashemi et al., 2016; Lee et al., 2016), or to power single-use diagnostic devices (Fraivan and Choi, 2016). The state of the art in the field of paper-based MFCs is summarized in Table S1 in the Supplementary information. In most of these studies, additional expensive materials are required, such as Nafion, used as a proton exchange membrane (Fraivan et al., 2014; Hashemi et al., 2016) and chemicals, such as ferricyanide, used as an electron acceptor at the cathode (Fraivan et al., 2014, 2013; Fraivan and Choi, 2016, 2014; Hashemi et al., 2016). These paper-based MFCs are constructed from multiple elements and materials (Choi et al., 2015; Lee et al., 2016), which may lead to manufacturing complexity. They also appear to be

restricted by short operational times (typically 20–200 min) (Fraivan et al., 2014, 2013; Fraivan and Choi, 2016). Finally, some studies refer to the use of pure cultures such as *Shewanella oneidensis* MR-1 (Wang et al., 2013; Yang et al., 2016b) further adds to the complexity of the system and is not compatible with practical in-field applications (Fraivan et al., 2013). All these aspects highlight the need for cheap, easy-to-use and robust paper MFC devices.

In this context, we report here the first single-component paper MFC, with the aim of developing a functional, yet simple, light and cost-effective single-use sensing device. The device is fabricated by screen-printing carbon-based electrodes onto a single sheet of paper. It is membrane-less, as the paper substrate itself acts as the separator between the two electrodes. Moreover, there is no need for sample pumping, since capillary forces in the paper create autonomous microfluidics that can be manipulated by changing the paper structure, thus tuning the performance of the device. In contrast to typical paper-based electrochemical sensors reported (Desmet et al., 2016), the paper MFC sensor does not require the use of an external potentiostat and, consequently, of an AC power supply, thus leading to an extremely light and easy-to-transport sensing tool.

In this work, we cross-linked the cellulose fibers within the paper based MFC, with glyoxal (a common cross-linking agent (Xu et al., 2002)), in order to increase robustness and operational lifetime of the device. The resulting MFC device has an extremely simple and easy-to-fabricate design, and, most of all, it is prepared from fully biodegradable components.

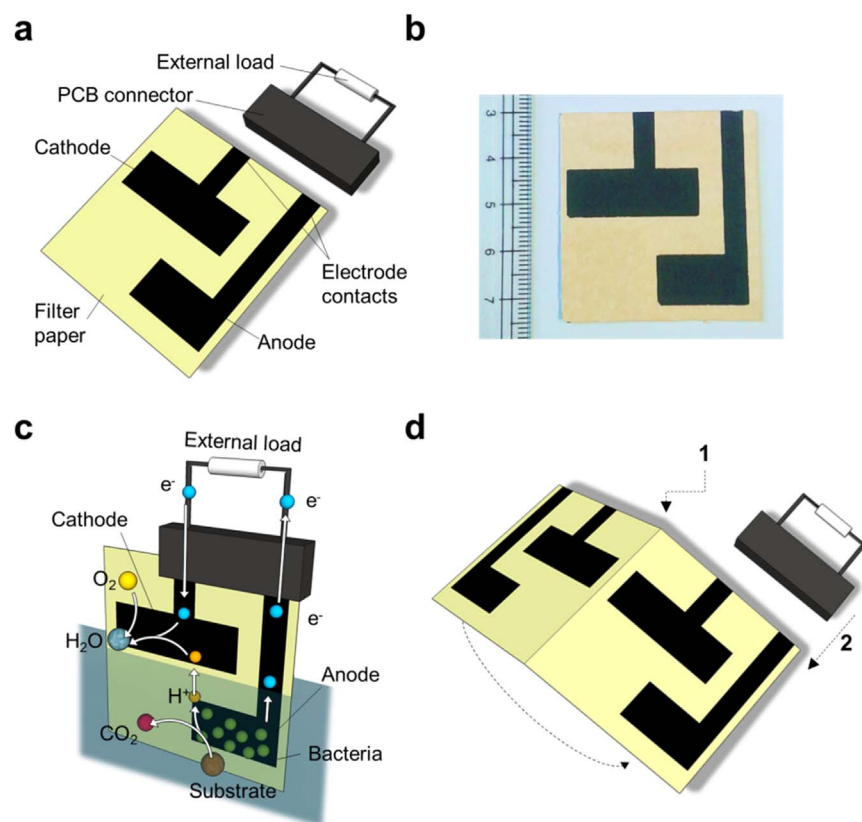


Fig. 1. (a) Schematic of the pMFC and electrical connection; (b) Photograph of the actual pMFC, showing size; (c) Principle of operation of the pMFC; and (d) Assembly of the fpMFC by folding two pMFCs back-to-back (1), with parallel electrical connection (2).

We then investigate the electrochemical performance of the paper-MFC and test its capability as a sensor for toxicants in water. In particular, to allow ready comparison with previous work, formaldehyde was used as a model bioactive compound, since it is a toxicant widely used for testing MFC-based sensors. Finally, we report on increased baseline current and enhancement of the sensor sensitivity by the simple design modification of folding two paper MFCs back-to-back, electrically connected in parallel.

2. Experimental section

2.1. Device fabrication

Single component paper-based MFCs (pMFC) were fabricated by screen-printing a conductive ink onto a single sheet of paper (Fabriano 5 HP). The conductive ink consisted of 20 mg α -cellulose (C8002, Sigma Aldrich) dissolved in 1 g of organic electrolyte solution, which consisted of 1-ethyl-3-methylimidazolium (EMIMAc, Sigma Aldrich) and dimethyl sulfoxide (DMSO, Sigma Aldrich) (92:8% w/w ratio). Conductive components, 40 mg carbon nanofibers (PR-24-XT-HHT, Pyrograf Products Inc., USA) and 40 mg graphite powder (< 20 μ m, 282863, Sigma Aldrich) were dispersed in this solution. Initially, half of the conductive materials were dispersed into the solvent mixture with a probe sonicator (microtip probe 6.3 mm ID, Fisher Scientific) for 30 s (5 s ON/OFF cycle), then half of the cellulose was added and the paste was stirred overnight using a magnetic stirrer, after which, the remaining powder mass was added to the paste and thoroughly dispersed using a pestle and mortar. Three layers of the conductive ink were screen-printed (43–80 μ m mesh) onto the paper to form the electrodes, Fig. 1. Each layer was printed, the entire sheet submerged in methanol for 20 min to phase invert the cellulose binder and displace the EMIMAc/DMSO solvent, and the sheet air-dried. The pMFC devices were then washed and soaked in water overnight. The electrode loading was found to be 1.85 ± 0.84 mg cm⁻², obtained experimentally by measuring the difference in mass of 1×1 cm samples of blank unprinted substrate paper versus samples of paper completely covered by with the printed electrode.

To cross-link the cellulose fibers in the pMFC, the devices were submerged for 3 h in aqueous solutions of glyoxal of varying concentrations, 0–24% w/v at room temperature (20 ± 3 °C), removed and heated at 140 °C for 1 h in an oven to effect reaction. This resulted in degrees of cross-linking corresponding to 0–94.8 mg g_{paper}⁻¹, as confirmed by HPLC analysis (Table S2). The conductivity of the resulting electrodes was 48.9 ± 1.9 Ω sq⁻¹.

To prepare electrodes with chitosan coatings, the anode was immersed in a 0.1% w/v chitosan (Sigma Aldrich) dissolved in 2% v/v acetate solution, prior to glyoxal cross-linking. The chitosan solution functioned as both the anti-solvent and source of chitosan. The electrodes were then washed three times for 30 min in water to remove any residual solvents. The conductivity of the resulting electrodes was 45.6 ± 2.7 Ω sq⁻¹.

2.2. Device material characterisation

All characterisation of the paper samples was performed in triplicate. The conductivity of the electrodes was determined by the four-terminal probe method running a cyclic voltammogram between 0.01 and -0.01 V with a 5 mV s⁻¹ scan rate using an Ivium Compactstat 104 (B08084, Ivium Technologies, NL) on the electrode surface. The tensile strength of the pMFCs was measured on an Instron 3369 (Instron, UK), using 1×10 cm pre-wetted paper strips (thoroughly wetted by soaking in deionised water overnight). The degree of cross-linking of the cellulose fibers was determined by measurement of glycolic acid post treatment, as previously described (Schramm and Rinderer, 2000): cross-linked paper samples (0.4 g accurately weighed) were treated with 5 mL of 4 M NaOH at 100 °C for 25 min; the extract

diluted by a factor of 10 and filtered through a 0.2 μ m nylon filter before HPLC analysis was performed (Shimadzu Class-VP HPLC with an Aminex HPX-87H column thermostated at 50 °C 15 min isocratic elution with 10 mM H₂SO₄ at a flow rate of 0.6 mL min⁻¹; UV-vis. detection at 210 nm). A calibration curve of peak area versus glycolic acid concentration was constructed (Fig. S1), and the glycolic acid concentration was determined (Eq. (1)):

$$\text{Glyoxal concentration (mg g}_{\text{paper}}^{-1}) = \frac{PA - b}{a \times DF \times WOF_{\text{ini}}} \times 0.7632 \quad (1)$$

Where PA is the peak area, a and b are the gradient and intercept of the line of best fit in the calibration, and DF the dilution factor which takes into account the volume of the hydrolytic reaction (mL), WOF_{ini} is the initial weight of the Fabriano paper (g), and $M_{\text{R}}(\text{glyoxal})/M_{\text{R}}(\text{glycolic acid}) = 0.7632$ (Schramm and Rinderer, 2000).

2.3. Biofilm analysis

A Jeol JSM-6480LV scanning electron microscope (SEM) was used to characterise the morphology of the fixed biofilm onto the electrode surface after enrichment and operation. The biofilm was fixed by following the procedure previously described (Chouler et al., 2017), which is also reported in the Supplementary information. All samples were coated with Au prior to imaging.

To assess the relative growth of the biofilm, crystal violet staining was performed (Merritt et al., 2015): after 24 h exposure of the anode to artificial wastewater and anaerobic sludge 0.5×0.7 cm electrode samples were excised and placed in 24 well plates. Samples were washed twice with 100 mM phosphate buffer solution (PBS) to remove non-attached bacteria and dried for 1 h at 50 °C. Crystal violet solution (1 mL 0.1% v/v) was added and the samples developed at room temperature for 30 min, the stain removed and the samples washed 3 times with 100 mM PBS. To dissolve the dye, 1 mL pure ethanol was added per sample and, following a 10-fold dilution in water, the absorbance measured at 590 nm.

2.4. Operation of the paper-based MFCs

Artificial wastewater (AW) containing (per litre of deionized water): 0.27 g (NH₄)SO₄, 0.06 g MgSO₄·7H₂O, 6 mg MnSO₄·H₂O, 0.13 g NaHCO₃, 3 mg FeCl₃·6H₂O, 4 mg MgCl₂, 3.1 g NaH₂PO₄·H₂O, 10.9 g Na₂HPO₄ and 10 mM potassium acetate (COD = 950 ± 32 mg/L) was used as the carbon source for the bacteria. The media was autoclaved and purged with nitrogen before being fed to the pMFCs. A printed circuit board (PCB) edge connector (TE Connectivity, UK) was used to connect the MFC anode and cathode to a voltmeter (ADC-24 Pico data logger, Pico technology, UK) and voltage, V , was continuously monitored under closed circuit conditions by applying an external load, R_{ext} , of 1 k Ω to polarize the cell. The resultant current (I) was calculated using Ohm's law ($I = V/R$) and the power, P , calculated as $P = VI$. To achieve enrichment of electrochemically active bacteria at the anode, the pMFCs were submerged in a sealed 100 mL vessel containing 10% v/v anaerobic sludge (provided by Wessex Water from a wastewater treatment plant in Avonmouth, UK), which was magnetically stirred (Fig. S2). The pH of the solution was 7.5 ± 0.1 and the conductivity 7.14 ± 0.15 mS cm⁻¹. Ten percent of the solution was replaced daily with freshly prepared AW. Once a stable current was observed, the pMFCs were fed with AW containing 10 mM potassium acetate, but no anaerobic sludge. To increase the output current whilst occupying the same operational space, two pMFCs were folded back-to-back and connected to a single PCB edge connector (Fig. 1d). The resulting device was named fpMFC. All studies were performed in triplicate.

2.5. Electrochemical analysis

After enrichment, electrochemical analysis of the fuel cells was

performed using an Autolab PGSTAT128N (Metrohm, UK), with the cells left at open circuit for up to 2 h beforehand to allow a steady state open circuit potential to develop. All electrochemical tests were performed with the anode as the working electrode and the cathode as the counter electrode. Polarisation curves were recorded in two electrode mode using a scan rate of 5 mV s^{-1} . Electrochemical Impedance Spectroscopy (EIS) was conducted over a frequency range of 50 kHz down to 0.1 Hz, using 10 steps per decade, with a sinusoidal perturbation of 10 mV amplitude, and an integration time set to 0.125 s, 3 cycles, using the anode as the working electrode, the cathode as counter electrode and an Ag/AgCl reference electrode. The latter was placed close to the anode through the injection port of the vessel (see Fig. S2). To determine the efficacy of proton diffusion within the pMFC, cyclic voltammetry, in two electrode mode at a scan rate of 5 mV s^{-1} and a potential window of -0.7 to 0.7 V , was used. Only the anode of the pMFC was submerged in a solution of 5 mM ferricyanide in 50 mM phosphate buffer and 100 mM NaCl solution.

2.6. Toxicant analysis

A toxic event was mimicked by exposing the MFCs to a solution of 0.1% v/v formaldehyde, by adding 1 mL concentrated formaldehyde solution (10% in AW) into the 100 mL incubation vessel. The current decay after exposure is defined as the initial rate of change of the current with respect to time, dl/dt , taken by the initial slope of the current response curve within the first 10 min of toxicant exposure. The delay time is defined as the time between the introduction of a toxicant and the first response from the MFC and the response time is defined as the time taken to reach 95% of the new steady state current after a toxic event.

3. Results and discussion

3.1. Device fabrication

Single component, air-breathing, paper-based MFCs (pMFCs) were fabricated by screen-printing, using fully biodegradable materials. Fig. 1a shows a schematic of the device, while its actual size is shown in Fig. 1b.

Firstly, the device fabrication was optimized. In particular, to increase the paper tensile strength, improve its robustness and enhance the operational lifetime of the device, the cellulose fibers in the paper and the cellulose in the ink binder of the pMFC were cross-linked by reaction with glyoxal (a common cross-linking agent (Xu et al., 2002)). Various degrees of cross-linking were evaluated and the greatest improvement in the tensile strength of the pMFC was achieved with $32 \text{ mg g}_{\text{paper}}^{-1}$ of glyoxal (Fig. S3), yielding a greater than threefold improvement versus non-treated paper, from $0.38 \pm 0.33 \text{ MPa}$ to $1.28 \pm 0.09 \text{ MPa}$ (Table S2). Increased levels of cross-linking had no further beneficial effects on the tensile strength of the paper. Thus, this degree of cross-linking was considered optimal to yield reproducibly cross-linked materials, and was used for all the subsequent tests.

The electrochemical performance, in terms of electron transfer capability, of the screen-printed device, before and after the cross-linking step, was investigated by cyclic voltammetry (CV) in a 5 mM ferricyanide solution used as a redox system (Fig. S4). The non-cross-linked device exhibited a very low current with no evidence of oxidation or reduction peaks over the potential range -0.7 to 0.7 V . On the other hand, the cross-linked device showed oxidation and reduction peaks at 0.34 V and -0.5 V respectively within the same potential range. As evidenced from the scanning electron microscopy (SEM) images of the electrodes (Fig. 2), the cross-linking treatment affects the porous structure of the electrode. In particular, by cross-linking the

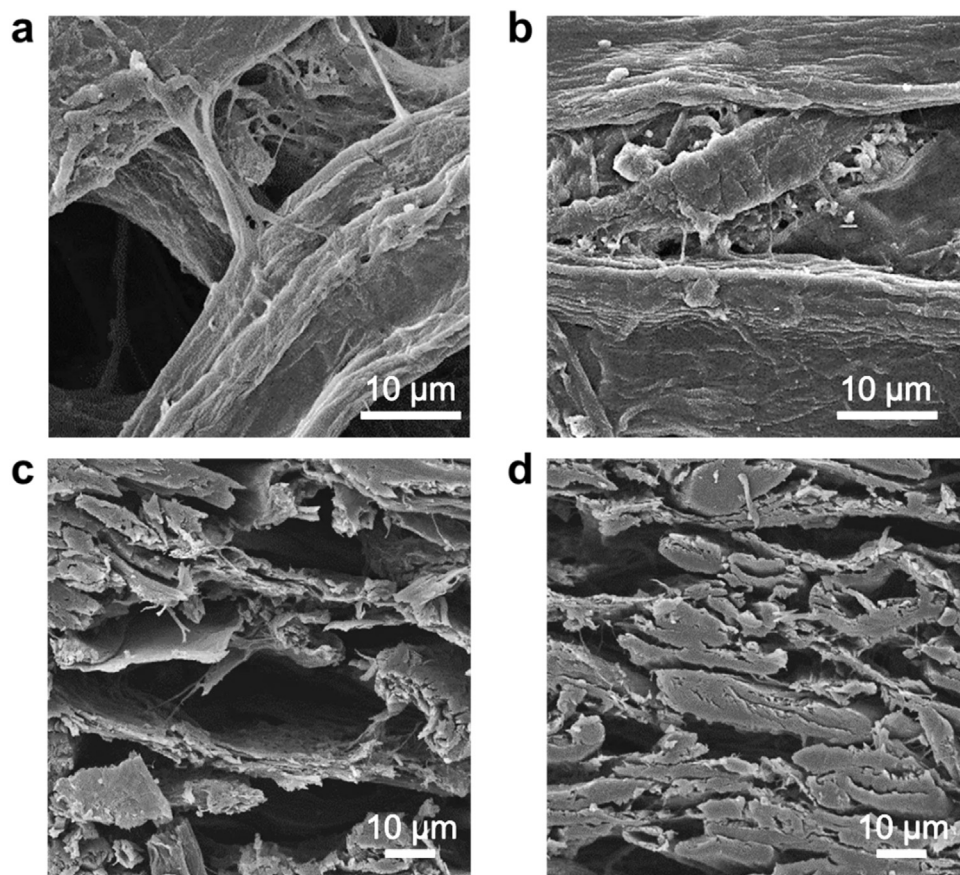


Fig. 2. SEM images of: (a) paper surface after cross-linking, (b) un-crosslinked paper, (c) electrode cross section after cross-linking, (d) un-crosslinked electrode cross section.

cellulose binder, a more open structure in the dried ink is maintained, and shrinkage and collapse is reduced. It is hypothesized that this open structure facilitates diffusion through the electrodes, as well as between the two electrodes, since the paper porosity is similarly enhanced. Indeed, it has been previously demonstrated that the increase in pore size of an electrode separating layer leads to greater power generation in MFCs by lowering its internal resistance (Zhang et al., 2010).

The electroactive surface area (EA) per geometric area (GA) of the resulting electrode, calculated using the Randles-Sèvečik equation (Fig. S5 in the Supplementary information), was estimated to be 0.5. Such low EA/GA fractions are common in paper-based carbon electrodes (Mateos et al., 2017).

3.2. Microbial fuel cell operation

The screen-printed device was subsequently tested as a microbial fuel cell. To this purpose, the electrodes were connected to a 1 k Ω resistor to polarize the cell, and the output voltage was continuously monitored. The electrode, acting as the anode, was submerged in a beaker containing artificial wastewater, with 10% v/v anaerobic sludge and 10 mM potassium acetate as a carbon source (Fig. S2), while the cathode was exposed to air. Fig. 1c shows the working principle of the pMFC. The organisms in the anodic biofilm catalyze the oxidation of acetate (the fuel) generating electrons (e⁻) and protons (H⁺). The electrons are transferred to the anode and move across the external circuit, while the solvated protons diffuse through the paper to the cathode. Here, the reaction is completed with the reduction of oxygen into water. No external membrane is required and the paper itself acts as a separator.

The current generated by the pMFC over time was monitored over a period of 8 days (Fig. 3) and after 4 days of operation, a steady state current of $0.18 \pm 0.04 \mu\text{A cm}^{-2}$ was achieved.

No appreciable current was generated through a control test in which the screen-printed device, sans sludge enriched anode, was incubated with AW and the signal measured with the electrodes connected to a 1 k Ω resistor (data not shown).

To investigate the effect of stacking the pMFCs, two pMFCs were folded back-to-back (device hereafter named fpMFC) and enriched as described above for the single pMFC. After six days of operation, the electrochemical performance of both the pMFC and the fpMFC was investigated by linear sweep voltammetry (LSV) and electrochemical impedance spectroscopy (EIS). Analysis of the power curves (Fig. 4a), polarisation curves (Fig. 4b) and impedance curves (Fig. 4c) thus obtained, suggest significantly enhanced performance for the fpMFC versus the single cell pMFC (Table S3).

The open circuit voltages (OCV) measured for pMFC and fpMFC were $68 \pm 13 \text{ mV}$ and $39 \pm 8 \text{ mV}$ respectively. These OCV values are much lower than for other MFC devices, which are typically in the range of 0.7–1.0 V (Ieropoulos et al., 2010). These values are also an order of magnitude lower than other MFCs with paper-based electrodes (ranging from 302 to 550 mV), which variously use screen-printed carbon electrodes on paper operated in a two chamber configuration (Fraivan and Choi, 2016), have a combination of a carbon veil anode with a conductive ink cathode (Winfield et al., 2015), or utilize a separator such as Nafion (Hashemi et al., 2016) or parchment paper (Lee et al., 2016). Thus, it appears likely that the absence of a membrane in the pMFC is responsible for the lower OCVs obtained in this study, due to oxygen diffusion to the anode. This drawback is, however, counteracted by the advantage of screen-printing the whole device (or multiple devices) onto a single piece of paper using a single ink formulation (and thus single screen), which hugely simplifies its manufacture and reduces cost, facilitating mass production. The slightly lower OCV of the fpMFC when compared to the pMFC (a difference of 29 mV) may be due to some loss in voltage via voltage reversal when electrically stacking MFC units, which has been widely reported (Ieropoulos et al., 2010; Ledezma et al., 2013; Oh and Logan, 2007).

Analysis of the polarisation curves, suggests that mass transfer limitations dominate over other losses in the cell (Fig. 4b), in agreement with the performance of other paper-based MFCs reported (Fraivan et al., 2016; Winfield et al., 2015).

To probe the effects of cross-linking more closely, images of the microbial biofilm developed on the electrode surface after enrichment (after 10 days of operation) were examined. The open structure generated by cross-linking provides greater surface area for the biofilm allowing the bacteria to colonize the pores of the electrode (Fig. S6).

It was hypothesized that enhancing formation of a biofilm on the anode surface, would lead to improved power performance of the device. Chitosan, has been reported to allow immobilization of whole cells onto surfaces (Rinaudo, 2006) and has been employed to enhance biofilm attachment onto electrode surfaces (Antolini, 2015; Higgins et al., 2011; Lau et al., 2008). To assess the efficacy of this strategy in these pMFCs, devices were prepared with anodes coated with a layer of chitosan (cpMFC) and bacterial colonization after 24 h of incubation, compared with that of non-treated anodes. SEM images of the samples (Fig. 5) show a visibly greater biofilm attachment for the case of the cpMFC. Moreover, crystal violet staining confirmed that the relative growth of the biofilm was over 5 times greater when using a chitosan layer on the anode (1.6% versus 8.7% relative growth (Fig. S7)). Despite the promise for increasing the biofilm attachment at the electrode, the electron transfer ability of the cpMFC device was poor, as confirmed by CV analysis (Fig. S8). This behavior was attributed to the presence of amine groups in chitosan that may hinder the diffusion of protons between the two electrodes, thus hindering the electrochemical performance of the device (Antolini, 2015).

Stacking two devices together (fpMFC) led to a maximum power density of $0.07 \pm 0.01 \mu\text{W cm}^{-2}$, over 1.7 times the value obtained with a single cell. Moreover, the current density generated at the maximum power output of the fpMFC was $3.0 \pm 0.6 \mu\text{A cm}^{-2}$, over 4 times greater than that of the pMFC. The enhanced performance of the fpMFC might be a consequence of the lower internal resistance: $2.2 \pm 0.4 \text{ k}\Omega$ for the fpMFC versus $5.7 \pm 0.8 \text{ k}\Omega$ for pMFC, (Fig. 4c). It has been previously shown that, when electrically connecting MFC units in parallel, the internal resistance of the overall system decreases, since the system tends towards the lowest common denominator (Papaharalabos et al., 2015). High internal resistances are usually observed in small-scale MFCs (Choi et al., 2011; Qian et al., 2009).

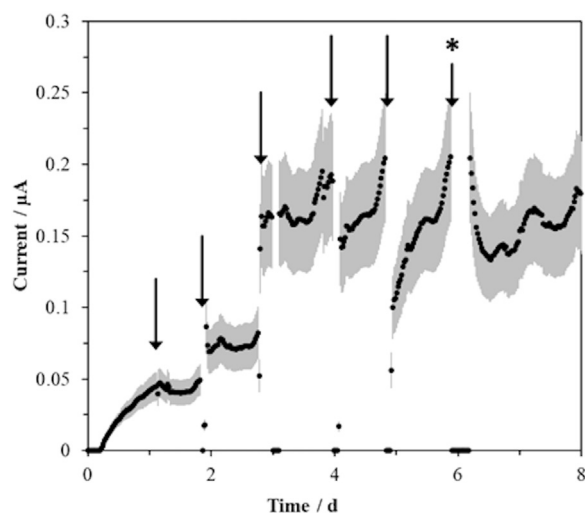


Fig. 3. Enrichment of pMFC. Arrows indicate replacement of 10% of the feed with fresh AW containing 10 mM potassium acetate and no anaerobic sludge. At almost 6 days (indicated with a *) electrochemical analysis (linear sweep voltammetry and electrochemical impedance spectroscopy) was performed. The decrease in current noted after each addition of nutrient medium (indicated by arrows) was due to minor disruptions of the pMFC feed solution during media replacement. Error bars (referring to experiments conducted in triplicate) are indicated by grey shaded region.

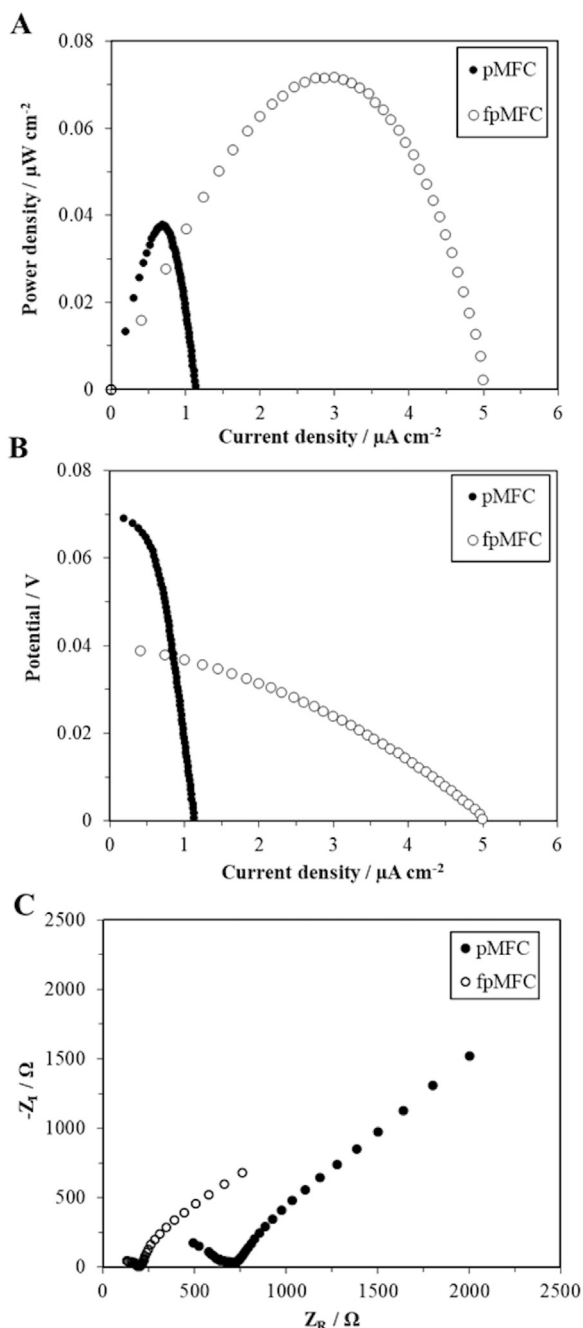


Fig. 4. (a) Power and (b) polarisation curves for the pMFC and fpMFC. Power and current densities refer to the geometric anodic electrode area: 2 cm^2 . (c) Comparison of electrochemical impedance spectroscopy curves for the pMFC and fpMFC.

Nonetheless, the internal resistances of both pMFC and fpMFC are almost one order of magnitude lower than similar air cathode paper-based MFC devices (Lee and Choi, 2015; Lee et al., 2016).

3.3. Biosensing capability-detection of formaldehyde

The response of both the pMFC and fpMFC to the presence of 0.1% v/v formaldehyde added to AW as a shock dose was subsequently investigated (Fig. 6). In both cases, exposure to the toxic compound caused a marked drop in the current output. In particular, the rates of current decay within the first 10 min of exposure had absolute values of $0.011 \mu\text{A min}^{-1}$ and $0.021 \mu\text{A min}^{-1}$ for the pMFC and fpMFC (Table S4). The greater response of the fpMFC reflects its enhanced sensitivity (Jiang et al., 2015). After 4 h of exposure, the steady state currents were

$-0.03 \mu\text{A}$ and $-0.15 \mu\text{A}$, representing an absolute total current drop of $0.3 \mu\text{A}$ and $0.6 \mu\text{A}$ for pMFC and fpMFC respectively. The current outputs reached negative values after 175 min and 115 min (for pMFC and fpMFC respectively) of exposure, thus indicating that the biofilm was severely affected by continuous exposure to the toxicant, in agreement with other studies (Dávila et al., 2011; Wang et al., 2013; Yang et al., 2016b). The nature of the response of these devices to formaldehyde suggests that the pMFC and fpMFC would suit shock sensor applications for water quality monitoring (Liu et al., 2014). The total response times (defined as the time taken to reach 95% of the steady state current after the toxic event) were 165 min (pMFC) and 200 min (fpMFC), which is much faster than other MFC biosensors subjected to the same shock (0.1% formaldehyde): $> 200 \text{ min}$ for a 140 μL single chambered MFC (Yang et al., 2016b) and $> 9.7 \text{ h}$ for a 120 mL single chambered MFC, Table S5 (Wang et al., 2013).

Thus, our work shows that, not only is the output current enhanced by simply folding two pMFCs back-to-back, but that the sensing performance of the overall system also improves. This result suggests a simple route to further optimize the biosensor, which does not compromise the simplicity of the device or complicate its manufacture.

The pMFC demonstrated appreciable reproducibility particularly in terms of electroactive response to the presence of formaldehyde. Nonetheless, the output current is lower than other MFCs reported in the literature. A way to increase the current signal could be by improving the oxygen reduction reactions (ORR) at the cathode. This is often done with platinum (Martin et al., 2011), however, recently more sustainable and cost-effective biomass derived ORR catalysts have been suggested (Chouler et al., 2016). Finally biofilm development could be enhanced by poisoning the potential of the anode to encourage electroactive biofilm development during enrichment, or through use of other material treatments to enhance the biofilm attachment at the anode (e.g. addition of polypyrrole or polyaniline) (Zou et al., 2009).

4. Conclusions

To conclude, in this work we report the first single component paper-based MFC with an extremely simple design and demonstrate the proof-of-concept of its use as a biosensor for toxicants in water.

Taking biodegradability, resource efficiency and cost as key design parameters, a screen-printed MFC was designed, which was built wholly of carbon based materials, with no metals in the disposable part of the device (the MFC itself). The natural biopolymer, cellulose, constitutes the bulk of the material: the paper upon which the device is constructed. Cellulose is also the ideal binder for the metal free conductive ink that constitutes the electrodes and allows proton transport by diffusion, thus obviating the need for a synthetic polymer membrane. The single component nature of the device ensures that a single chemical cross-linking step, using an agent that adds only the elements C, H and O, may be used to enhance the robustness of the MFC and maintain the porous nature of both paper and electrodes. Post use, should the MFC be discarded, it will biodegrade, leaving no trace, including no metal residues. Concerns about potential microbial contamination of the environment may be addressed by either incinerating the MFC, or disposing of the MFC in the same manner as human waste. The ease of power output scale-up of the device was demonstrated by folding two paper MFCs back-to-back and electrically connecting them in parallel, thus paving the way for stacking opportunities to enhance performance.

Finally, the potential of the devices as rapid onsite shock sensors for water quality assessment, particularly for detection of bioactive compounds in water, was demonstrated. Indeed, effective water quality monitoring is currently limited by either expensive, time consuming and offsite analytical methods that need to be performed in the laboratory, or by field test kits that have a limited reliability and high cost (Chouler and Di Lorenzo, 2015). The implementation of our paper-based MFC biosensor for water quality monitoring can provide a

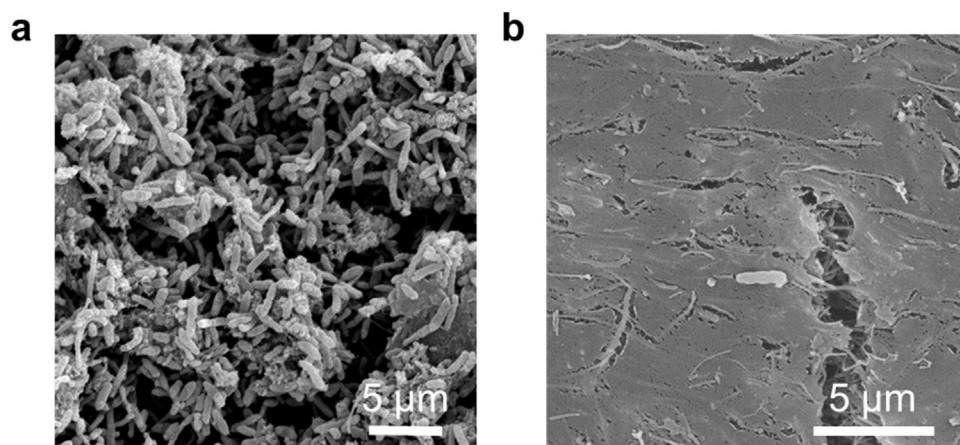


Fig. 5. SEM images of the anode surface after 24 h inoculation in AW, containing 10% v/v anaerobic sludge for: (a) cpMFC; (b) pMFC. In both cases the anodes were connected to the cathode through a 1 k Ω external resistor and the cell voltage was monitored.

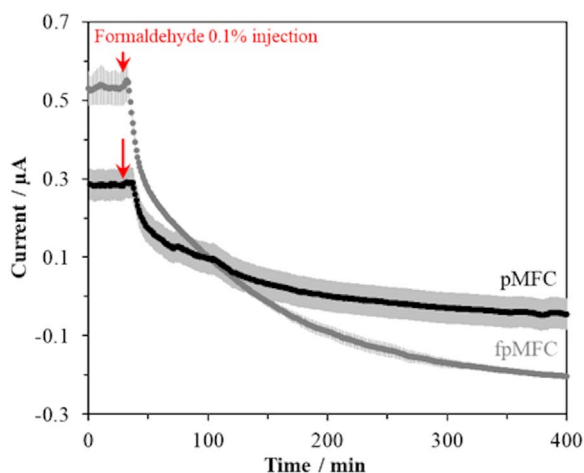


Fig. 6. Amperometric response of the pMFC and fpMFC to an injection of 0.1% v/v formaldehyde. The grey shaded region refers to the error between three measurements.

solution to detecting toxic compounds in water that is easy to operate by submersion into the sample to be analyzed, simple to manufacture and is extremely cheap. Taking into account the materials specified in the experimental section, the estimated cost of the pMFC device is £0.43. This value could be significantly reduced by upscaled manufacturing and all processes, including printing, phase inversion (solvent bath), and cross-linking are amenable to roll to roll manufacture. Moreover, with careful design, there is scope for the MFC to be easily deployable in remote locations with data acquisition, analysis and even potentiostatic control possible using a mobile device (e.g. mobile phone) (Delaney et al., 2013; Lin et al., 2015).

In real scenarios, the performance of the pMFC might be susceptible to environmental conditions, such as temperature, pH and conductivity (Peixoto et al., 2011), which should be simultaneously monitored and integrated in the sensor response. This principle has been recently demonstrated in the field of MFC based toxicant biosensors by calibrating the MFC output signal to a reference MFC in simultaneous operation (Yang et al., 2016a).

Practical applications would also require pre-enrichment of the anodes of the pMFCs with electroactive bacteria. Indeed such a technique has previously been demonstrated to provide a functional working voltage with paper based MFCs within just 35 min (Winfield et al., 2015).

The distributed water quality monitoring that this device could enable would be of particular value in developing countries, where water and resources are extremely limited, and the need for water monitoring devices, that are cheap, simple to manufacture, and easy to dispose of, is clear. As such, our single-use device, which offers

portability, facile use, and biodegradability, has the potential to improve the way water quality is monitored. It can provide those in remote and poor areas a way to quickly, simply and cost-effectively analyze water supplies that are critical to their health, livelihood security and wellbeing.

Acknowledgments

The authors would like to thank: Zuhayr Rymansab and Pejman Iravani from the Department of Mechanical Engineering, University of Bath, for assistance and help on the design of the pMFC; Carlos César Bof Bufon, from the Brazilian Nanotechnology National Laboratory (LNNano) in Campinas for fruitful discussions; Wessex Water for providing anaerobic sludge; Elizabeth Bevon from the EPSRC Centre for Doctoral Training in Sustainable Chemical Technologies, University of Bath, for assistance with CV experiments. We thank Sally Gaden, Bath City College, for advice on screen printing. Funding from the Engineering and Physical Sciences Research Council (EPSRC) and the EPSRC Centre for Doctoral Training in Sustainable Chemical Technologies (EP/P510907/1; EP/G03768X/1; EPSRC EP/L016354/1) is acknowledged.

Appendix A. Supporting information

Supplementary data associated with this article can be found in the online version at <http://dx.doi.org/10.1016/j.bios.2017.11.018>.

References

- Allen, R.M., Bennetto, H.P., 1993. *Appl. Biochem. Biotechnol.* 39, 27–40.
- Antolini, E., 2015. *Biosens. Bioelectron.* 69, 54–70.
- Choi, G., Hassett, D.J., Choi, S., 2015. *Analyst* 140, 4277–4283.
- Choi, S., Lee, H.-S., Yang, Y., Parameswaran, P., Torres, C.I., Rittmann, B.E., Chae, J., 2011. *Lab Chip* 11, 1110–1117.
- Chouler, J., Bentley, I., Vaz, F., O'Fee, A., Cameron, P.J., Di Lorenzo, M., 2017. *Electrochim. Acta* 231, 319–326.
- Chouler, J., Di Lorenzo, M., 2015. *Biosensors* 5, 450–470.
- Chouler, J., Padgett, G.A., Cameron, P.J., Preuss, K., Titirici, M.-M., Ieropoulos, I., Di Lorenzo, M., 2016. *Electrochim. Acta* 192, 89–98.
- Dávila, D., Esquivel, J.P., Sabaté, N., Mas, J., 2011. *Biosens. Bioelectron.* 26, 2426–2430.
- Delaney, J.L., Doeven, E.H., Harsant, A.J., Hogan, C.F., 2013. *Anal. Chim. Acta* 803, 123–127.
- Desmet, C., Marquette, C.A., Blum, L.J., Doumèche, B., 2016. *Biosens. Bioelectron.* 76, 145–163.
- Fraiwani, A., Choi, S., 2014. *Phys. Chem. Chem. Phys.* 16, 26288–26293.
- Fraiwani, A., Choi, S., 2016. *Biosens. Bioelectron.* 83, 27–32.
- Fraiwani, A., Kwan, L., Choi, S., 2016. *Biosens. Bioelectron.* 85, 190–197.
- Fraiwani, A., Lee, H., Choi, S., 2014. *IEEE Sens. J.* 14, 3385–3390.
- Fraiwani, A., Mukherjee, S., Sundermier, S., Lee, H.-S., Choi, S., 2013. *Biosens. Bioelectron.* 49, 410–414.
- Hashemi, N., Lackore, J.M., Sharifi, F., Goodrich, P.J., Winchell, M.L., Hashemi, N., 2016. *Technology* 4, 98–103.
- Higgins, S.R., Foerster, D., Cheung, A., Lau, C., Bretschger, O., Minteer, S.D., Neelson, K., Atanassov, P., Cooney, M.J., 2011. *Enzym. Microb. Technol.* 48, 458–465.

- Ieropoulos, I., Greenman, J., Melhuish, C., 2010. *Bioelectrochemistry* 78, 44–50.
- Jiang, Y., Liang, P., Zhang, C., Bian, Y., Yang, X., Huang, X., Girguis, P.R., 2015. *Bioresour. Technol.* 190, 367–372.
- Lau, C., Cooney, M.J., Atanassov, P., 2008. *Langmuir* 24, 7004–7010.
- Ledezma, P., Greenman, J., Ieropoulos, I., 2013. *Bioresour. Technol.* 134, 158–165.
- Lee, H., Choi, S., 2015. *Nano Energy* 15, 549–557.
- Lee, S.H., Ban, J.Y., Oh, C.-H., Park, H.-K., Choi, S., 2016. *Sci. Rep.* 6, 28588.
- Lin, F.-T., Kuo, Y.-C., Hsieh, J.-C., Tsai, H.-Y., Liao, Y.-T., Lee, H.-C., 2015. *IEEE Sens. J.* 15, 3751–3758.
- Liu, B., Lei, Y., Li, B., 2014. *Biosens. Bioelectron.* 62, 308–314.
- Di Lorenzo, M., Curtis, T.P., Head, I.M., Scott, K., 2009. *Water Res.* 43, 3145–3154.
- Di Lorenzo, M., Thomson, A.R., Schneider, K., Cameron, P.J., Ieropoulos, I., 2014. *Biosens. Bioelectron.* 62, 182–188.
- Martin, E., Tartakovsky, B., Savadogo, O., 2011. *Electrochim. Acta* 58, 58–66.
- Mateos, R., Alonso, R., Escapa, A., Morán, A., 2017. *Materials* 10, 79.
- Merritt, J., Kadouri, D.E., O'Toole, G.A., 2015. *Curr. Protoc. Microbiol.* 1–29.
- Mulchandani, A., Kaneva, L., Chen, W., 1998. *Anal. Chem.* 70, 5042–5046.
- Oh, S.-E., Logan, B.E., 2007. *J. Power Sources* 167, 11–17.
- Ongley, E.D., 2001. *Water Int.* 26, 14–23.
- Palaniappan, M., Gleick, P.H., Allen, L., Cohen, M.J., Christian-Smith, J., Smith, C., 2010. *Clearing the Waters: A Focus on Water Quality Solutions*. Oakland, CA, USA.
- Papaharalabos, G., Greenman, J., Melhuish, C., Ieropoulos, I., 2015. *Int. J. Hydrog. Energy* 40, 4263–4268.
- Peixoto, L., Min, B., Martins, G., Brito, A.G., Kroff, P., Parpot, P., Angelidaki, I., Nogueira, R., 2011. *Bioelectrochemistry* 81, 99–103.
- Potter, M.C., 1911. *Proc. R. Soc. B Biol. Sci.* 84, 260–276.
- Qian, F., Baum, M., Gu, Q., Morse, D.E., 2009. *Lab Chip* 9, 3076–3081.
- Rinaudo, M., 2006. *Prog. Polym. Sci.* 31, 603–632.
- Sarpong Adu-manu, K., Tapparello, C., Heinzelman, W., Apietu Katsriku, F., Abdulai, J., 2017. *ACM Trans. Sens. Netw.* 13, 1–41.
- Schramm, C., Rinderer, B., 2000. *Anal. Chem.* 72, 5829–5833.
- Stein, N.E., Hamelers, H.V.M., Buisman, C.N.J., 2010. *Bioelectrochemistry* 78, 87–91.
- Vaiopoulou, E., Melidis, P., Kampragou, E., Aivasidis, A., 2005. *Biosens. Bioelectron.* 21, 365–371.
- Wang, X., Gao, N., Zhou, Q., 2013. *Biosens. Bioelectron.* 43, 264–267.
- Winfield, J., Chambers, L.D., Rossiter, J., Greenman, J., Ieropoulos, I., 2015. *J. Mater. Chem. A* 3, 7058–7065.
- WWAP (United Nations World Water Assessment Programme), 2015. *The United Nations World Water Development Report 2015: Water for a Sustainable World*. Paris.
- Xu, G.G., Yang, C.Q., Deng, Y., 2002. *J. Appl. Polym. Sci.* 83, 2539–2547.
- Yang, W., Wei, X., Choi, S., 2016a. *IEEE Sens. J.* 16, 8672–8677.
- Yang, W., Wei, X., Fraiwan, A., Coogan, C.G., Lee, H., Choi, S., 2016b. *Sens. Actuators B Chem.* 226, 191–195.
- Yetisen, A.K., Akram, M.S., Lowe, C.R., 2013. *Lab Chip* 13, 2210–2251.
- Zhang, X., Cheng, S., Huang, X., Logan, B.E., 2010. *Energy Environ. Sci.* 3, 659–664.
- Zhao, W., van den Berg, A., 2008. *Lab Chip* 8, 1988–1991.
- Zou, Y., Pisciotta, J., Billmyre, R.B., Baskakov, I.V., 2009. *Biotechnol. Bioeng.* 104, 939–946.